EARTH SURFACE PROCESSES AND LANDFORMS
Earth Surf. Process. Landforms **43**, 765–778 (2018)

Published online 17 November 2017 in Wiley Online Library
(wileyonlinelibrary.com) DOI: 10.1002/esp.4239

Proglacial erosion rates and processes in a glacierized catchment in the Swiss Alps

Ian Delaney,[1]* Andreas Bauder,[1] Matthias Huss[1,2] and Yvo Weidmann[1]
[1] Laboratory of Hydraulics, Hydrology and Glaciology (VAW), ETH-Zürich, Zürich, Switzerland
[2] Department of Geosciences, University of Fribourg, Fribourg, Switzerland

Received 13 October 2016; Revised 22 August 2017; Accepted 23 August 2017

*Correspondence to: Ian Delaney, Laboratory of Hydraulics, Hydrology and Glaciology (VAW), ETH-Zürich, Zürich, Switzerland. E-mail: delaney@vaw.baug.ethz.ch

ESPL
Earth Surface Processes and Landforms

ABSTRACT: In the Swiss Alps, climatic changes have not only caused glacier retreat, but also likely increased sedimentation downstream of glaciers. This material either originates from below the glacier or from periglacial environments, which are exposed as glaciers retreat, and often consist of easily erodible sediment. Griesgletscher's catchment in the Swiss Alps was examined to quantify erosion in the proglacial area, possible hydrological drivers and contributions of the sub- and periglacial sources. Digital elevation models, created from annual aerial photographs, were subtracted to determine annual volume changes in the proglacial area from 1986 to 2014. These data show a strong increase in proglacial erosion in the decade prior to 2012, coincident with increasing proglacial area size. However, examination of the gradient between discharge and sediment evacuation, and modeled sediment transport, could suggest that the proglacial area began to stabilize and sediment supply is limited. The large influx of sediment into the proglacial reservoir, which is roughly 2.5 times greater than the amount of sediment eroded from the proglacial area, demonstrates the importance of subglacial erosion to the catchment's sediment budget. Although far more sediment originates subglacially, erosion rates in the proglacial area are over 50 times greater than the rest of the catchment. In turn, both sub- and periglacial processes, in addition to constraining sediment supply, must be considered for assessing future sediment dynamics as glacier area shrinks and proglacial areas grow. © 2017 The Authors. Earth Surface Processes and Landforms published by John Wiley & Sons Ltd.

KEYWORDS: periglacial processes; glacial sediment; alpine sediment dynamics; alpine hydrology; glacier retreat

Introduction

Glaciated catchments are characterized by exceptional amounts of sediment transport and erosion compared to their fluvial counterparts (e.g. Hallet *et al.*, 1996; Einsele and Hinderer, 1997). Sediment production rates in the Alps are only surpassed by other glaciated regions in Alaska and Central Asia (Hallet *et al.*, 1996). In Switzerland, the passage of both sediment and water through glaciated catchments is of utmost interest as much of the runoff is used for hydropower production, so changes in the discharge of water and sediment can greatly affect infrastructure and water resource management (Schaefli *et al.*, 2007). A substantial increase in sedimentation has been observed in the Alps in recent decades (e.g. Hinderer *et al.*, 2013; Micheletti *et al.*, 2015; Lane *et al.*, 2016) and has proved troublesome for hydropower companies, who must manage reduced reservoir capacity and increased sediment flushing, along with higher amounts of abrasion by sediment passing through turbines and other equipment (e.g. Auel and Boes, 2012; Felix *et al.*, 2013; Hinderer *et al.*, 2013).

On both short and geological timescales glaciers are extremely effective at altering landscapes (e.g. Hallet *et al.*, 1996; Meigs *et al.*, 2006; Herman *et al.*, 2015), and their ability to erode is enhanced during periods of perturbation such as warming and glacial retreat (e.g. Hallet *et al.*, 1996; Anselmetti *et al.*, 2007; Koppes and Montgomery, 2009; Koppes *et al.*, 2009), which the region is currently undergoing (e.g. Huss *et al.*, 2015). The material expelled from the catchment originates either subglacially or periglacially (e.g. Fenn and Gomez, 1989; Mao *et al.*, 2014; Guillon *et al.*, 2015). Additionally, supraglacial and englacial sediments, often deposited on or in the ice, are not negligible, as melted out material can be deposited in the proglacial area (e.g. Eyles, 1979). Subglacial sediment production is largely thought to be controlled by abrasion of bedrock, plucking and quarrying of material by regelation of materials on the lee side of bedrock bumps, and activation of sediment already beneath the glacier (e.g. Alley *et al.*, 1997; Swift *et al.*, 2005; Beaud *et al.*, 2016). New periglacial areas form as glaciers retreat and are often a rich source of sediment available for transport by fluvial or mass-wasting activity (e.g. Church and Ryder, 1972; Fenn and Gomez, 1989; Warburton, 1990; Ballantyne, 2002a); however, the relative contribution of periglacial and subglacial sediment to total sediment discharge in a catchment varies greatly between basins (Fenn and Gomez, 1989; Mao *et al.*, 2014; Guillon *et al.*, 2015).

Geomorphic processes responsible for increases in periglacial sediment transport often occur following glacier retreat and before the landscape has stabilized. They include gully and channel formation and hill-slope failure of moraines

that are no longer buttressed by ice (e.g. Ballantyne, 2002a; Werder *et al.*, 2010; Porter *et al.*, 2010; Lane *et al.*, 2016). These processes, and their propensity to transport large amounts of sediment quickly, can be attributed to the loose nature of the recently uncovered sediment, and the ease with which it can erode via fluvial (e.g. Warburton, 1990) or mass-wasting processes (e.g. Porter *et al.*, 2010; Legg *et al.*, 2014). The time until the landscape stabilizes is largely a product of sediment exhaustion in the area, and can occur well after the complete disappearance of glaciers (e.g. Ballantyne, 2002a; Carrivick and Heckmann, 2017). For instance, in the Swiss Alps, proglacial gulley formation following the 'Little Ice Age' around the year 1850 reached a maximum in the 50 years following deglaciation, with infill of the gullies and stabilization occurring up to 140 years after deglaciation (Curry *et al.*, 2006), demonstrating the landscape's prolonged response following glacier retreat and the propensity for increased sediment yield to be an enduring issue for infrastructure.

As the volume of ice in Switzerland is expected to strongly decrease within the next half-century (e.g. Huss, 2012), observed changes to sediment dynamics (e.g. Hinderer *et al.* 2013; Micheletti *et al.*, 2015; Lane *et al.*, 2016) will undoubtedly evolve. Glacier retreat will result in the exposure of expanses of landscape, likely covered with plentiful amounts of glacial drift available for transport (e.g. Church and Ryder, 1972; Fenn and Gomez, 1989; Warburton, 1990; Ballantyne, 2002a; Lane *et al.*, 2016). Additionally, hydrology in glaciated catchments will change; in the short term increased melt will lead to higher glacier discharge, however, on longer timescales, reduced ice-cover will result in less ice melt and runoff (e.g. Farinotti *et al.*, 2012). Hydrological forecasts until 2100 suggest that reduced average and peak runoff volumes will limit sediment transport, as the amount of time below the critical erosion threshold will increase (Raymond-Pralong *et al.*, 2015). However, this study did not account for increased sediment supply caused by the reduction in glacier cover, growth of proglacial areas or the effects of subglacial sediment.

Given the expected exposure of great amounts of sediment during the forthcoming deglaciation, examining the interaction between hydrology, glacier morphology and sediment erosion and deposition around glaciers is key to understanding future erosion and sedimentation in Switzerland. Previous work has shown that decadal-scale atmospheric warming results in increased erosion in alpine environments (Micheletti *et al.*, 2015; Micheletti and Lane, 2016), although future reduced stream flows may hinder the ability of this water to transport sediment (Raymond-Pralong *et al.*, 2015). Additionally, sediment exhaustion models serve as a framework to assess the duration and propensity of erosion (Ballantyne, 2002a; Curry *et al.*, 2006; Lane *et al.*, 2016), although not at an annual resolution. Without knowledge of the evolution of the sediment erosion, determining the timescales over which a landscape responds to deglaciation is not possible. In order to characterize sediment processes in glaciated catchments, the amounts of subglacial erosion must be quantified. Quantification of annual-scale volume changes, the relationship of proglacial sediment dynamics with runoff, sediment transport capacity and glacier morphology, and an estimate of the proportion of subglacial and periglacial erosion, will help determine the landscape response to growth of proglacial areas. In turn, the importance of factors that evolve with retreat of glaciers, such as the availability of transportable sediment, morphology of the proglacial area and evolution of hydrology can be examined.

To better determine these quantities and assess processes, Griesgletscher in the Swiss Alps is examined. This medium-sized glacier lies above a hydropower reservoir, and the retreat of the glacier beyond the reservoir margin in 1986 exposed a new proglacial area. Due to its proximity to hydropower infrastructure, the catchment has been thoroughly monitored for glacier mass balance, and aerial photographs have been collected annually.

Volume changes in Griesgletscher's proglacial area for nearly each year from 1986 to 2014 are deduced by creating digital elevation models (DEMs) from aerial photographs. Additionally, by comparing observed volume and elevation changes in the proglacial area with morphology of the proglacial area, reservoir bathymetry, and with modeled catchment hydrology and transport capacity, this paper aims to assess sediment processes in the proglacial area. By examining the evolution of proglacial erosion, hydrological drivers of erosion, and proportions of this eroded sediment from subglacial and periglacial sources, this research provides more insights into the relationship between hydrology and sediment transport, the availability of transportable sediment and the stability of the proglacial area, as glaciers retreat and regional hydrologic patterns evolve.

Study Site

Griesgletcher lies close to the main ridge of the Alps and the water divide of the Rhone, Rhine and Po rivers (Figure 1A). The lower end of the roughly 10 km^2 catchment is constrained by a dam, creating a hydropower reservoir, Griessee (Figure 1B), in which the glacier terminated until 1986. The catchment was 51% glacierized in 2007 with a single sub-catchment draining to the reservoir from the east. Its maximum elevation is 3370 m above sea level (a.s.l.), with the glacier terminating at roughly 2450 m a.s.l. in 2014. Retreat beyond the reservoir margin since 1986 has exposed a proglacial area (about 600 m long in 2014), which is largely sediment covered, with three longitudinal bedrock ridges that channelize glacier runoff (Figure 2). Given the simplistic catchment area and glacier morphology, recent exposure of formerly ice-covered sediments, a long history of glacier mass balance measurements and aerial photographs associated with the hydropower infrastructure, the Griesgletcher catchment proves ideal for examination of sediment dynamics in glaciated catchments.

Data

For determining erosion rates and processes in Griesgletscher's proglacial area, DEMs were created with photogrammetric techniques, and catchment runoff was reconstructed with a glacier mass balance model. Creation of these original datasets required aerial photographs, temperature and precipitation data, and coarse digital elevation models of the catchment. Additionally, bathymetric data of the Griessee were utilized to determine catchment erosion rates.

DEMs were created from aerial photos that were collected annually from 1986 to 2014, with the exceptions of 1993 and 2004. From 1986 to 2010, aerial frame photographs of the proglacial area were acquired by swisstopo between late August and the middle of October of each year. The original photogrammetrical negatives were scanned by swisstopo and private companies using a photogrammetrical scanner with a resolution of 14 μm. Publicly available camera calibration information, such as fiducial marks, focal length, principal point and radial distribution, was implemented for all photographs. Images from 2011 to 2014 were collected from

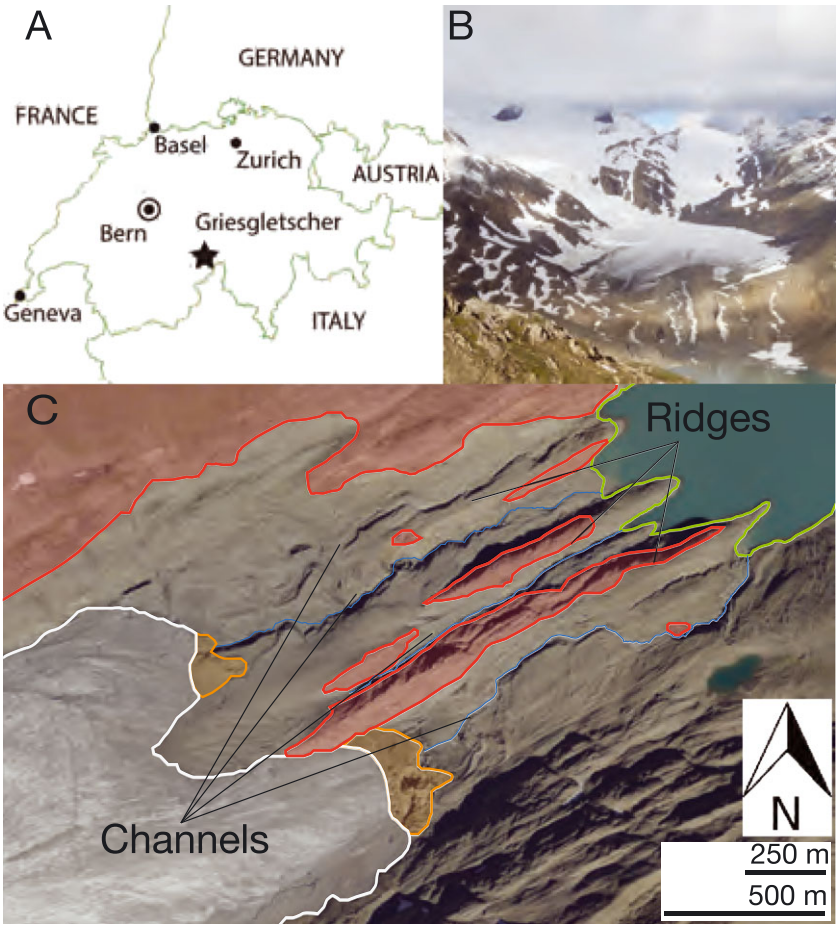

Figure 1. (A) Geographic location of Griesgletscher in southern Switzerland. (B) Oblique photo from July 2017 of Griesgletscher with proglacial area and reservoir. (C) Orthorphoto of Griesgletscher's proglacial area in fall 2014 with features in the proglacial area. Channels and ridges are labeled. The red lines denote approximate location of bedrock. Orange lines show potentially debris-covered ice. The white line is approximate glacier extent and blue lines are streams. The green line is the approximate reservoir boundary. [Colour figure can be viewed at wileyonlinelibrary.com]

aerial scan strips by Leica ADS-40 and ADS-80 cameras from swisstopo.

Modeling of catchment runoff required temperature and precipitation data as inputs as well as 25 × 25 m DEMs of the glacier surface. The model was run with hourly temperature data collected at Ulrichen (1350 m a.s.l.; 8 km from the glacier) and precipitation data from Piotta (1000 m a.s.l.; 26 km from the glacier). Climate data from other nearby stations were available; however, datasets from Ulrichen and Piotta correlated best with observed summer ablation and winter accumulation of Griesgletscher (Huss *et al.*, 2009). Additionally, six DEMs of the glacier surface and extent were utilized in the modeling from 1986, 1991, 1998, 2003, 2007 and 2012 (Bauder *et al.*, 2007).

Measured discharge, determined by the reservoir's water level and supplied by the hydropower operator, and glacier mass balance were used to calibrate the mass balance model. As water leaves the glacier through multiple channels, direct measurements of discharge are impossible. Mass balance measurements on Griesgletscher have been conducted annually since 1961 (Huss *et al.*, 2009). Winter accumulation measurements were collected in the spring of each year by snow soundings and snow density measurements since 1994, and summer ablation was constrained by a network of semi-permanent stakes across the glacier.

Bathymetries of the proglacial reservoir collected in 1976 (exact date not available), 2011 (11 September), 2013 (21 September) and 2014 (21 October) were provided by internal reports by the hydropower operator, OFIMA, and were used to determine sedimentation rates in the reservoir. As the recent bathymetries were collected in the fall of the corresponding year, they are largely coincident with the collection of aerial photographs; for instance, both the 2013 bathymetry and aerial photographs capture reservoir sedimentation and proglacial erosion that occurred during the 2013 melt season. The last three bathymetries used multi-beam echo soundings, which more accurately account for nuanced topography compared to a single-beam method. As some of the current reservoir volume was taken up by the glacier in the 1976 survey, only the estimated region gathered in both 2011 and 1976 is considered for comparison. Here, the bathymetry data are used to estimate the contributions of proglacial and subglacial erosion and corroborate trends in catchment erosion.

Methods

Determining changes in the proglacial area

Photogrammetry has been used in several contexts for investigating glacial processes, such as changes in glacier volume (e.g. Reinhardt and Rentsch, 1986), spatial variations in mass balance (e.g. Hubbard *et al.*, 2000) and subglacial drainage (e.g. Rippin *et al.*, 2003; Fischer *et al.*, 2005), as well as periglacial processes (e.g. Schiefer and Gilbert, 2007; Micheletti *et al.*, 2015). To assess elevation changes in the

proglacial area, DEMs were constructed every year from 1986 to 2014, with the exception of 1993 and 2004, through photogrammetric techniques.

Photographs were internally calibrated using camera information discussed above. Two to four images were combined to make a photogrammetrical block using five to six marked ground control points visible in photographs across all years, for interannual coregistration and a large number of tie points. An aero-triangulation of each block was applied to calculate the external orientation parameter for each image (X, Y, Z, roll, pitch, yaw). Leica Photogrammetrical Suite software created point clouds from the resulting block. To counteract the effects of shadowing, point clouds were manually enhanced with stereo editing tools by adding additional points and break-lines in low-contrast regions, such as on the lee sides of ridges and gullies, enhancing sharpness and quality of the DEM. Additionally, these point cloud data were used to create an orthorectified mosaic for each year. Swisstopo conducted the orientation of the scan strips from 2012 to 2014; thus the calibrations discussed above were not necessary. However, a large blunder was noted on the lee sides of a gully in the swisstopo DEMs and masked out.

Photogrammetrically derived point clouds were interpolated on a colocated 2 × 2 m grid, for increased processing speed and to smooth the effects of potential spikes and troughs in the point cloud, and elevation change was calculated by subtracting the DEMs from subsequent years. As Nuth and Kääb (2011) discuss, a reference area or control area can account for differences and offsets when comparing different DEMs. For each image pair we designated between 8 and 20 control areas throughout the study area (Figure 2A) (Betts *et al.*, 2003; Schiefer *et al.*, 2007). In more recent years we were able to find stable areas within the proglacial area on bedrock ridges to use as control areas; however, in earlier years these were unavailable as they were covered by the glacier or were not yet stable. Additionally, reference areas on stable rock on opposing sides of the proglacial area, and in the middle when ice free, and consistent across all years were used to estimate errors and level of detection.

Elevation differences over the control areas were assumed to be zero and the mean elevation change over the control areas was considered to be the systematic offset between the two DEMs. To account for this systematic error, the mean elevation change was subtracted during the next iteration of the DEM differencing:

$$\Delta z_a = \Delta z_i - \overline{\Delta z_{con}} \tag{1}$$

where Δz_a is the adjusted elevation difference from subtraction over the study area. Δz_i represents the initial elevation difference of DEM pixels without adjusting for systematic vertical misfit, and $\overline{\Delta z_{con}}$ is the mean elevation change over the control area by which the DEMs were co-registered.

The study area spanning the proglacial area (Figure 2) was bound on one side by the maximum lake extent observed in orthophotographs, which occurred in 2005. On the uphill side, the maximum glacier extent of the two years considered was used as a limit, ensuring that observed changes could be attributed to sediment movement as opposed to glacier ice melt. We calculated the erosion volume, ΔV, as

$$\Delta V = \sum_{n_{ff}} \overline{\Delta z_a} A \tag{2}$$

where A represents the area of a pixel, in this case 4 m^2, n_{ff} is the number of pixels in the proglacial area, and $\overline{\Delta z_a}$ is the average elevation change in the study area.

To provide error estimates we used methods described in Rolstad *et al.* (2009) to account for the spatial dependence on errors within the control areas. This method requires assessing an area over which errors between the DEMs are correlated (A_{cor}), by determining a correlation length (radius), L, determined by a semivariogram of the differenced control areas:

$$A_{cor} = \pi \cdot L^2 \tag{3}$$

A_{cor} varied greatly over the study period, but with an average value across all years of 2300 m^2 (average correlation length, L, of approximately 27 m).

The standard deviation in vertical error was determined by

$$\sigma_z = \pm \sqrt{\sigma^2_{\Delta ca} \cdot \frac{A_{cor}}{5 \cdot A_{pga}}} \tag{4}$$

where $\sigma_{\Delta ca}$ is the standard deviation in the elevation differences over the pixels within the control areas, A_{cor} is from Equation 3 and A_{pga} is the extent of the proglacial area. If A_{pga} is smaller than A_{cor}, then $\sigma_z = \sigma_{\Delta ca}$. To convert the error to a volumetric error over the proglacial area, σ_z, is multiplied by A_{pga}.

DEM errors and uncertainties

Photogrammetric techniques for creation of DEMs are prone to considerable errors, especially when compared to other methods such as terrestrial LiDAR (e.g. Bolstad, 1992; Baltsavias, 1999; James and Robson, 2012; Kenner *et al.*, 2014). Given the broad area that our study area covers (Figure 1), the relatively few available ground control points within aerial images and lack of reference areas from the unstable sediment or ice, these DEMs undoubtedly contain systematic errors. In addition to systematic errors in the DEMs, debris-covered ice and vague definition of the glacier's extent could lead to overestimates in erosion, by mistaking ice melt for sediment erosion (e.g. Bennett *et al.*, 2000; Schomacker and Kjær, 2008).

Systematic issues in the DEMs include bands or waves in the subtracted DEMs, tilt within the photo block and potentially poor resolution of the imagery (e.g. Fabris and Pesci, 2005), leading to errors in our subtractions. Given our lack of stable areas in the study area consistent throughout the study period (due to unconsolidated debris or glacier ice), creating distributed control points over which to correct images (e.g. Schiefer *et al.*, 2007; Micheletti *et al.*, 2015) or truthing the our DEMs to another dataset, such as a terrestrial LiDAR (e.g. Baltsavias, 1999; James and Robson, 2012; Kenner *et al.*, 2014), is not possible. However, for each image pair the vertical offset was determined by 8–20 control areas on stable terrain distributed throughout the proglacial area that we thought stable, discussed above, for which to co-register the DEMs (e.g. Fabris and Pesci, 2005; Betts *et al.*, 2003; Nuth and Kääb, 2011). Using this offset, errors in the DEMs were assessed by calculating offsets in the two reference areas (Figure 2A and Table I), although some control areas were contained within the reference areas, and a third reference area was added in the middle of the proglacial area following deglaciation. The mean offset of all pixels in the reference areas were less than 20 cm for all but 6 of the 25 sets of differenced DEMs; one set experienced offsets greater than 20 cm (1988–1987) (Table I). Field visits to these locations showed that it was underlain by bedrock and small amounts of vegetation not exceeding 5 cm in height, which is visually evident in color aerial photos, suggesting this area has been stable over the length of the study period (Sigler *et al.*, 2002). However, as these areas lie on steeper slopes, outside of the proglacial area, and on the margin of the photo

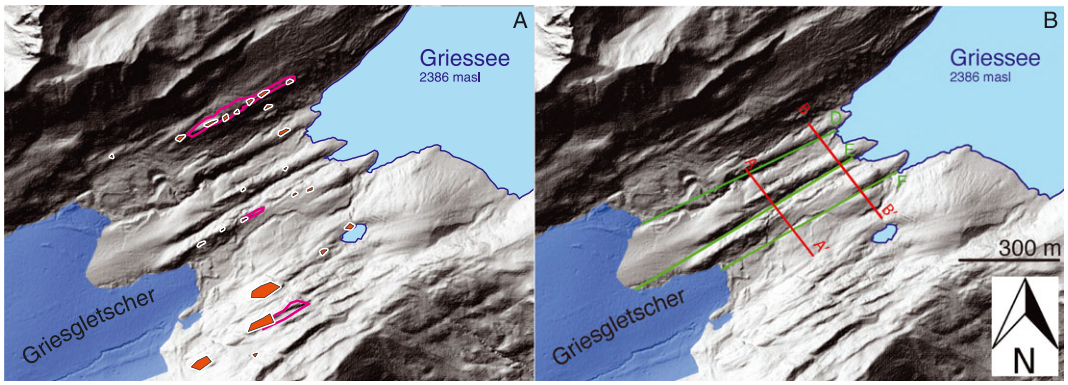

Figure 2. Overview of proglacial area with 2015 glacier extent in dark blue. Water bodies are in light blue. (A) Reference areas (purple) and control areas (orange). (B) Cross-sections are shown in red and longitudinal profiles are green. [Colour figure can be viewed at wileyonlinelibrary.com]

Table I. Relative level of detection (rLOD) at 90% confidence based upon 2014 DSM (Figure 2).

Image pair	rLOD	Control area offset	Corrected reference area offset
1987–1986	1.282 m	0.27 m	−0.08 m
1988–1987	1.417 m	0.32 m	−0.44 m
1989–1988	1.457 m	0.50 m	0.04 m
1990–1989	1.988 m	−0.47 m	−0.07 m
1991–1990	2.039 m	0.20 m	−0.02 m
1992–1991	1.601 m	−0.36 m	−0.29 m
1994–1992	1.547 m	0.75 m	−0.17 m
1995–1994	1.565 m	−0.14 m	0.02 m
1996–1995	1.405 m	−0.21 m	0.27 m
1997–1996	1.302 m	−0.03 m	−0.12 m
1998–1997	1.197 m	−0.20 m	0.20 m
1999–1998	1.229 m	0.22 m	−0.16 m
2000–1999	1.404 m	0.15 m	−0.02 m
2001–2000	1.434 m	−0.29 m	0.06 m
2002–2001	1.537 m	−0.18 m	0.08 m
2003–2002	1.482 m	0.43 m	−0.16 m
2005–2003	1.488 m	−0.15 m	0.08 m
2006–2005	1.526 m	−0.05 m	−0.04 m
2007–2006	1.353 m	0.29 m	−0.09 m
2008–2007	1.311 m	−0.15 m	0.11 m
2009–2008	1.526 m	0.35 m	−0.04 m
2010–2009	1.535 m	−0.02 m	−0.24 m
2011–2010	2.184 m	−0.30 m	−0.16 m
2012–2011	2.110 m	−0.21 m	0.26 m
2013–2012	1.074 m	−0.28 m	0.20 m
2014–2013	0.495 m[a]	−0.00 m	−0.02 m

[a] As these values are determined by comparison with 2014 DSM, the rLOD determined in 2014–2013 is low due to the assumption of zero error in the 2014 dataset.

block, these reference areas might not be representative of the entire proglacial area.

To determine the relative level of detection (rLOD) of each DEM subtraction, each DEM in the pair was compared to the 2014 reference area to determine the standard deviation. 2014 was selected as the reference DEM as it is believed to have the highest quality. Other studies (e.g. Schiefer *et al.*, 2007; Micheletti *et al.*, 2015) use ground control points to determine such errors; however, such points are not available in this study due to the dynamic nature of the study area. The rLOD with 90% confidence was determined by

$$\mathrm{rLOD} = \sqrt{(1.68)\sigma_a^2 + (1.68)\sigma_b^2} \quad (5)$$

where a and b are consecutive DEMs and σ is the standard deviation of the pixels in the reference areas of the two DEMs. The mean rLOD of our photo pairs with 90% confidence is roughly ±1.48 m, with the highest being ±2.18 m and the lowest 1.07 m (Table I), and agree with other studies using similar aerial photographs (e.g. Schiefer *et al.*, 2007; Micheletti *et al.*, 2015).

Retreating glaciers can exhibit a debris-covered tongue (e.g. Lundstrom *et al.*, 1993; Glasser *et al.*, 2016), which can make determining glacier extent difficult (e.g. Paul *et al.*, 2004). Field visits to Griesgletscher in summer 2016 confirmed that ice-cored debris exists in the proglacial area approximately 50 m from the bare ice of the glacier front on the flatter slopes on the southern area of the proglacial area. In areas of high erosion visible in Figure 1, particularly in areas close to the glacier

margin, orthophotos were examined to identify erosion processes such as gully formation, which could account for the elevation loss instead of ice melt. For instance, in some recent years high amounts of erosion are visible on the northwestern edge of the glacier (Figure 4). Although it is possible that some erosion here could be a product of ice melt, examination of orthophotos suggests gully formation in freshly exposed, unconsolidated sediment caused the large height change. Additionally, although some DEM subtractions seem 'patchy' (e.g. 2007–2008; Figure 4), it is assumed that such 'patchy' areas would be present in most years if debris-covered ice melt were common. Instead, most subtractions show channelized erosion, which is likely attributable to fluvial processes.

Glacier runoff, hydrology and sediment transport

To better understand the interaction of erosion of sediment in the proglacial area and catchment hydrology, the glacio-hydrological model GERM (Huss *et al.*, 2008) was implemented. Modeled runoff was needed as no catchment discharge measurements exist at the sub-monthly resolution. The model was run with hourly temperature and precipitation data (from 1 October 1983 to 1 October 2014) to produce hourly runoff estimates at the glacier snout, capturing sub-daily variations or peak discharges.

The model calculates the hourly distribution of accumulation and melt across the glacier surface on a 25 m grid. Snow accumulation is estimated from <1.5°C and precipitation increase with glacier elevation was parametrized with a linear gradient. An enhanced temperature-index model (Hock, 1999) computes snow and ice melt. Air temperatures are extrapolated to the glacier surface using a lapse rate of -5.47°C km^{-1}, derived from surrounding meteorological stations. Meltwater runoff from snow, firn and bare-ices area is routed through linear storage reservoirs whose retention constants were estimated from literature values (Farinotti *et al.*, 2012). For more details on the modeling procedure refer to Huss *et al.* (2008). Model parameters were calibrated by comparing model results to monthly discharge volumes measured in the reservoir and observed seasonal glacier mass balance data covering the study period.

To relate modeled runoff from the catchment directly to erosion in the proglacial area, we implemented methods developed by Rickenmann (2001) and used by Raymond-Pralong *et al.* (2015), which describe bedload transport capacity as a function of slope steepness, channel width and discharge above a critical threshold. Here, modeled runoff data were used and DEMs were used to determine slope (Table II). These widths were determined by examining orthophotos.

Critical discharge, q_c, at which bedload transport initiates, is described as

$$q_c = 0.065(s-1)^{1.67} g^{0.5} Dm_{50}^{1.5} \alpha^{-1.12} \quad (6)$$

with bed slope α, mean sediment size Dm_{50} in meters, and s the ratio between solid and fluid densities (2650 kg m^{-3}, 1000 kg m^{-3}, respectively). We used a value of 12 cm for Dm_{50} in Equation 6; this was an upper bound, discussed in Raymond-Pralong *et al.* (2015). Unit discharge of sediment, q_b, is calculated as

$$q_b = 1.5(q - q_c)_+ \alpha^{1.5} \quad (7)$$

where α is slope (m/m), q is water discharge per unit width and q_c is critical discharge. To account for macro-roughness a slope reduction is implemented based in part upon Dm_{84}, for which 84% of sediment is smaller than this size. α is reparametrized using methods discussed in Rickenmann and Recking (2011). These amounts are then scaled to the entire channel width to determine total sediment discharge. We used a range of values for Dm_{50} ranging from 3 cm to 15 cm, with Dm_{84} being 3–4 times larger.

Results and Discussion

Volume changes and morphology of the proglacial area

Our results suggest that 125 600 m^3 of material was removed from the proglacial area (which increased to a size of 0.21 km^2 by 2014) in the the 28-year period and was not replenished by material from other parts of the catchment (subglacial or periglacial). The uncertainty in this estimate, based upon the 90% confidence interval of the control areas, is roughly ±23% of the cumulative amount of material transported from the proglacial area. This erosion volume corresponds to an erosion rate of 5.4 cm a^{-1} in the proglacial area over the study period. Evacuation of material from the proglacial area is minimal at the beginning of the study period when the proglacial area is small. On average, only 1 930 (±630) m^3 of material is eroded annually over the first 10 years. However, the proglacial area experiences both greater net annual erosion as the proglacial area grows in size. Net annual erosion reached a maximum in 2012 when 20 100 (±2 240) m^3 of material was removed from the proglacial area (Figure 3).

Scaling volume changes to the size of the proglacial area results in the mean height change, or specific erosion rate. Early years of the study undergo erosion rates of over 1 m (Figure 3). This could be due to concentrated erosion while the proglacial area was small or the effect of the few pixels in the DEM subtraction. Additionally, glacier ice could remain in these areas, resulting in the great height changes (discussed below); however, due to the small extent, the volume contribution is minimal over these years. The erosion rates of the proglacial area remain relatively constant over the study period following high erosion rates found at the beginning of the study. Despite relatively steady erosion rates from the mid-1990s onward, the proglacial area's volume changes generally increase with time, suggesting that the quantity of

Table II. Mean slope of the profiles' proglacial area (PGA) (Figure 4).

Year	Mean slope (°)	PGA ΔH (cm a^{-1})
2000	9.6	-5
2001	12.9	-6
2002	9.6	-3
2003	8.0	-11
2005	9.6	-5
2006	9.1	-8
2007	9.6	-9
2008	8.0	-7
2009	7.4	-8
2010	9.1	-11
2011	8.5	0
2012	8.0	-11
2013	7.4	1
2014	7.4	0

Note: ΔH stands for mean elevation change.

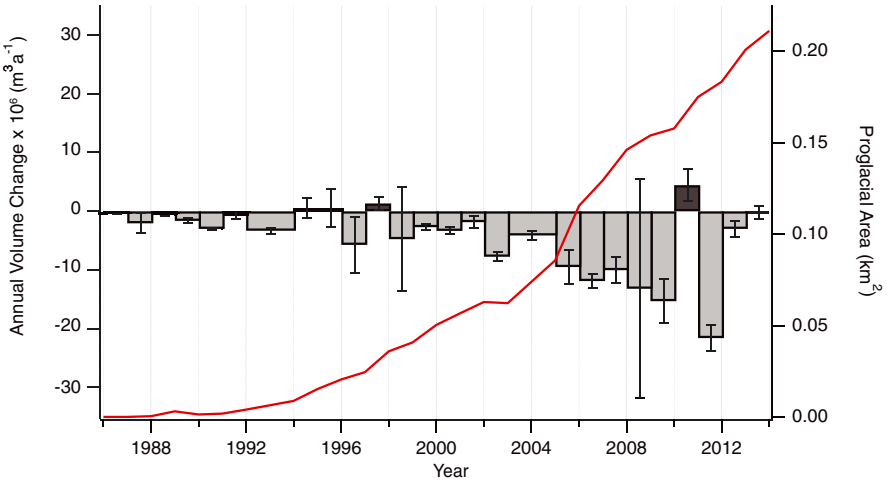

Figure 3. Annual volumetric change in the proglacial area. The red line denotes proglacial area size. Lighter (darker) bars represent negative (positive) volume or height changes corresponding to net erosion (deposition). Error bars in both panels correspond to 95% confidence intervals based on the uncertainty assessment. [Colour figure can be viewed at wileyonlinelibrary.com]

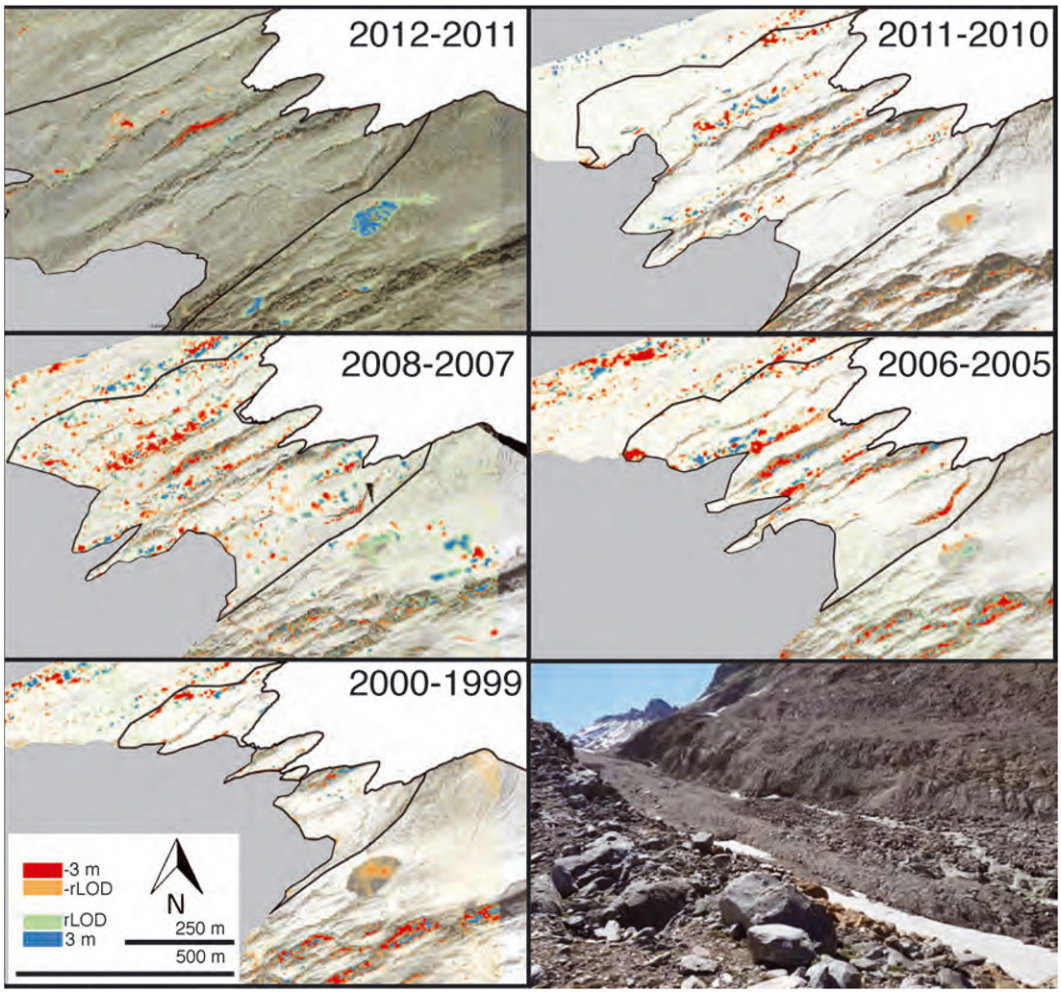

Figure 4. Significant DEM differences and orthophotos of selected years and oblique photo of proglacial area. Warm (cool) colors are negative (positive), representing erosion (deposition), and transparent areas are below the level of detection given in Table I. Reservoir and glacier have been masked out. Note the significant levels of height change in channelized areas. [Colour figure can be viewed at wileyonlinelibrary.com]

material transported out of the proglacial area over this time period is largely a result of greater area and thus availability.

Four of the 26 annual periods experienced net annual deposition in the proglacial area. However, only in 2011 does the net annual deposition lie within the 95% uncertainty range. The presence of deposition suggests that substantial subglacial sediment can be transported, and the amount of sediment from this source deposited in the proglacial area can exceed the amount eroded from the proglacial area.

Given the large specific erosion rates and volumes over the period of the study, it is quite possible that a substantial amount of the volume loss is due to melt of debris-covered

ice. This is especially relevant due to the recent deglaciation of the area. However, given the amount of bedrock underlying the proglacial sediment and the bedrock ridges, between which much erosion occurs (Figures 1 and 4), it seems that debris-covered ice may only be present in regions proximal to the glacier. Although aerial photographs may suggest that the lateral features in the proglacial areas are lateral moraines, these features are cored by bedrock (see oblique photos in Figures 1 and 4) and once were the bed of the glacier as opposed to a margin. Additionally, no wet sediment on channel walls has been identified on field visits. Lastly, it can be assumed that debris-covered ice melt would be relatively steady across most years, as the sensitivity to temperature changes under debris is dampened (e.g. Hoelzle and Haeberli, 1995; Nicholson and Benn, 2006); thus interannual variations in material loss are likely a result of sediment transport, although the quantity of material loss could be affected by ice melt.

Much erosion and deposition appears to occur in channelized areas within the proglacial area (Figure 4), as water leaves the glacier from a different combination of conduits over time (personal communication, M. Funk). Thus, should the height loss be attributable to erosion, as opposed to ice melt, the contribution of a particular channel in the proglacial area to total erosion varies over time, and new sediment sources can be accessed by meltwater. For instance, in the differenced DEMs 2007 and 2008, much erosion occurred in a channel on the southeast side of the proglacial area (Figure 4). This could be the result of a new outlet of the glacier meltwater, conceivably caused by changes in flow direction of water at the glacier bed following glacier retreat (e.g. Fischer *et al.*, 2005) and thus a new sediment-rich source. In some years, such as 2011–2012, large amounts of deposition appear to have occurred in a channel close to the glacier (Figure 4). Failure of channel walls could be a result of over-steepening by fluvial activity at the base of the channel or the result of debris-covered ice melt and loss of cohesion of wall material, or the mass loss could be due to ice melt. By either of the first two mechanisms or their combination, collapse of these surfaces could result in the filling of the channel bottom with sediment, providing the proglacial streams with a large supply of sediment. The subsequent relaxation of erosion in the last years of the study could be attributed to the stabilization of these processes, either by exhaustion of sediment supply or reduced amounts of ice-cored debris remaining in channels.

Cross-sections within the proglacial area show that much erosion and deposition occur in channels (Figure 5). Although it is possible that some differences in channel morphology could be due to the effects of flow stage, this is likely not the case as we estimate water depths in much of the catchment to be less than 1 m, below the rLOD (Table I), and less than the changes observed in channel bottoms in Figures 5 and 6. Interestingly, large amounts of deposition from 2010 to 2013 are visible (Figure 5B), likely deposition from 2011 (Figure 3). Erosion at the bottom of channels, collapse of channel walls and some erosion outside of channelized areas can be seen in the cross-sections. The presence of wall collapse suggests that some channel walls lie at their angle of repose. When erosion occurs at the channel base, temporarily increasing the slope, material can be readily replenished by failure of channel walls (e.g. Werder *et al.*, 2010).

To assess the influence of the proglacial area's slope on erosion rates, longitudinal profiles were created for years between 2000 and 2014. Mean slope was evaluated based on the distance from the lake to the glacier margin and the corresponding elevation difference (Figure 2B and Table II). The proglacial area was generally steeper early in the 2000s

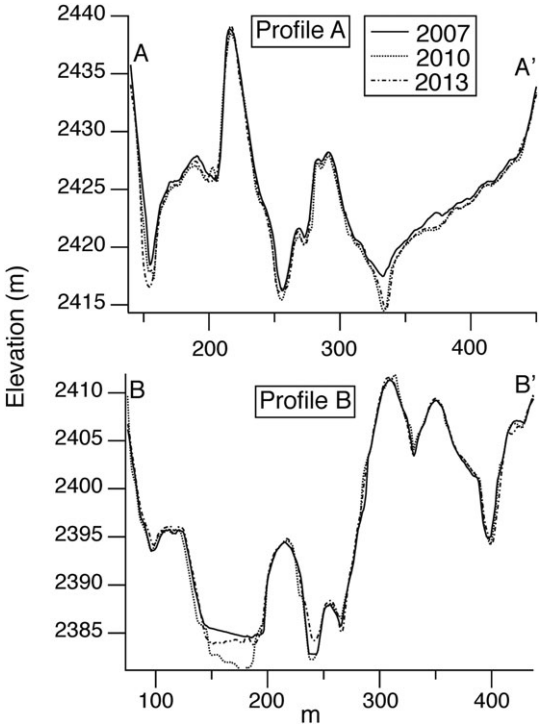

Figure 5. Cross-sections of the proglacial area, as seen in Figure 2B, downslope direction.

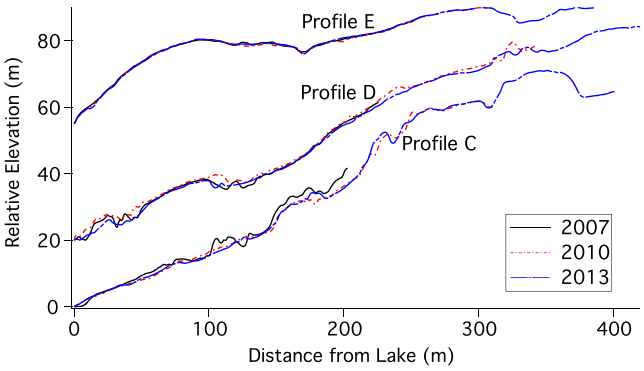

Figure 6. Longitudinal profiles from three select years. Profiles follow green lines in Figure 2B. Vertical axis represents relative elevation, with each profile originating at the lake level. Horizontal axis represents distance from lake. [Colour figure can be viewed at wileyonlinelibrary.com]

and slope decreased with time (Table I). However, in 2010, the year with the second most proglacial erosion, it experienced a higher slope than the year before, possibly due to deposition of sediment along the profile, which could have contributed to the substantial erosion that year. In more recent years, the decreasing slope could provide the means to slow water enough to enable the deposition observed in 2011 and reduced erosion in 2013 and 2014. Examination of selected longitudinal profiles (Figure 6) shows areas, particularly near the lake (profiles C and D), that are prone to large amounts of both erosion and deposition. The 2010 profiles (C and D) show several instances of localized deposition (Figure 6) in reaches closer to the lake, which could have been the result of channel collapse, thus providing some of the sediment necessary to cause the large amount of erosion in 2010.

Water and sediment

Although the relationship between erosion of sediment and runoff in a catchment is often complex, increased erosion is broadly correlated with warming and thus other processes such as glacier retreat and increased greater runoff (e.g. Stott and Mount, 2007; Leggat *et al.*, 2015; Micheletti *et al.*, 2015; Lane *et al.*, 2016). To better describe this relationship, modeled runoff data are implemented to examine annual hydrological characteristics (such as peak flow) in the ability of water to transport sediment and the evolution of sediment transport with respect to discharge.

To examine potential drivers of erosion, hydrological parameters derived from the hydrological model (i.e. total discharge, standard deviation in discharge and maximum discharge over timescales up to 1 week) were compared between proglacial change using a two-sample *t*-test. As no significant hydrological characteristics were found in years that experience deposition, it is possible that deposition is a result of depleted sediment supply in the proglacial area and only minimal deposition by subglacial sources. Alternatively, subglacial hydraulic conditions could be favorable in these years to evacuate large amounts of sediment, which are subsequently deposited in the proglacial area. These conditions include increased subglacial water pressure due to greater variability in meltwater input or variations in hydraulic gradient due to morphological changes to the glacier surface. Both processes moderate the velocity at which subglacial water flows, and thus the shear stress between the water and the subglacial sediment (e.g. Röthlisberger, 1972; Fowler and Walder, 1994).

The hydrology of years that experience more than 10 000 m^3 of sediment erosion suggests that they experience greater discharge quantities, discharge variability (standard deviation) and maximum discharge on timescales from 1 h to 1 week over the early season, and greater discharge over the entire season all with higher than 95% certainty. The importance of early-season hydrology compared to late-season hydrology could be due to reduced availability of sediment later in the season following the first high discharges in May and June which erode available sediment. Additionally, hill-slope processes and wall collapse, potentially supplying sediment channels bottoms, could occur early in the season, when meltwater from overlying snow can permeate sediment and reduce cohesive strength (e.g. Montgomery and Dietrich, 1994).

Initial examination of both cumulative amounts of erosion volumes and discharge over the study period (Figure 7) suggest that the relationship between sediment dynamics and runoff evolves substantially. Early in the study period, the volume change gradient with respect to discharge is not as high as compared to the long-term average. Following approximately 300×10^6 m^3 of discharge (1998), the gradient becomes greater and meltwater erodes more sediment, possibly due to the larger proglacial area and the increased sediment availability. The relationship of increasing volume loss with respect to discharge continued until between 635×10^6 and 700×10^6 m^3 of discharge (2010–2012) had passed through the proglacial area. Afterwards it appears that the relationship has returned to a gradient similar to that at the beginning of the study period. This could be attributed to further development and stabilization of gullies in the proglacial area, along with the evacuation of transportable sediment out of the proglacial area (Lane *et al.*, 2016). Although extrapolation of this trend into the future is flawed due to the few data points, it could be that a threshold amount of discharge has acted upon the proglacial area, and the proglacial area is beginning to stabilize and sediment availability is diminishing (e.g. Ballantyne, 2002b; Lane *et al.*, 2016; Carrivick and Heckmann, 2017).

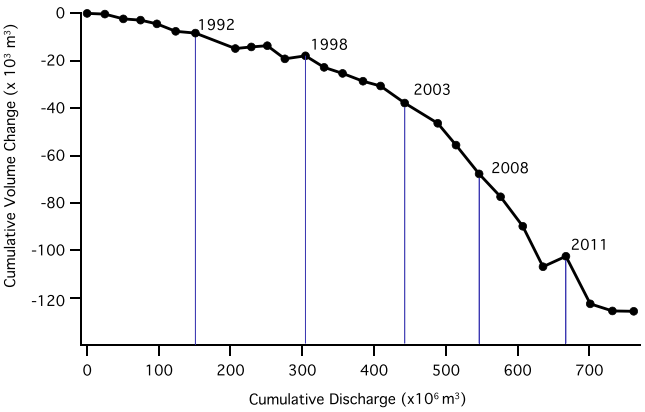

Figure 7. Cumulative relationship between eroded volume and discharge. [Colour figure can be viewed at wileyonlinelibrary.com]

Use of a sediment transport model, described above, can be used to link catchment hydrology with sediment dynamics via the process of bedload transport (e.g. Rickenmann, 2001). The relationship between sediment erosion in the proglacial area and erosion predicted by the model is minimal; however, some instances do occur. 2014, a year with negligible amounts of net erosion, also experienced lower modeled sediment discharge (Figure 3). However, 2011, a year that experienced sediment ,but experienced moderate modeled sediment discharge. Furthermore, many years that underwent higher levels of erosion compared to neighboring years also experienced higher modeled amounts of erosion compared to neighboring years (e.g. 2000–2001, 2002–2003 and 2006–2007). Most importantly, the modeled sediment discharge far overestimates the measured amount of proglacial erosion, with the exception of 2012–2012. Although many combinations of grain sizes were used, none correlated significantly even in rank and sediment discharge was overestimated by a large amount. This could be attributable to poor parametrization of parameters such as Dm_{50} and slope, for which the relationship is quite sensitive. For some model runs the slope reduction (Rickenmann and Recking, 2011) was excluded, leading to massive overestimates of sediment discharge, even with very large grain sizes.

Diminished sediment supply in the proglacial area could undoubtedly cause overestimation and lack of correlation in modeled sediment erosion given Equation 7, particularly in later years. This could be implied by the correlation of years with high erosion compared to neighboring years in both the modeling and observed datasets, whereby excess runoff is able to act upon additional sediment, not available in previous years. The discrepancy during 2010–2011, which experienced deposition, also suggests this. Additionally, modeled amounts of sediment transport were also overestimated to a greater degree at the beginning of the study period compared to more recent years. This could be due to limited access of sediment by meltwater during this time period due to reduced proglacial area size, compared to other periods of the study. When examining the longitudinal profiles (Figure 6), some steeper sections in profiles C and D appear to experience little erosion or deposition across the three datasets. Profile E largely represents an area that is not near an active channel and thus more stable. Increased potential sediment transport is directly related to slope (e.g. Meyer-Peter and Müller, 1948; Rickenmann, 2001), which has been updated for each time step based upon our DEM analysis. In Griesgletscher's proglacial area, this could result in relatively high amounts of erosion of sediment early in the deglaciation when slopes were higher (Table II), exhausting

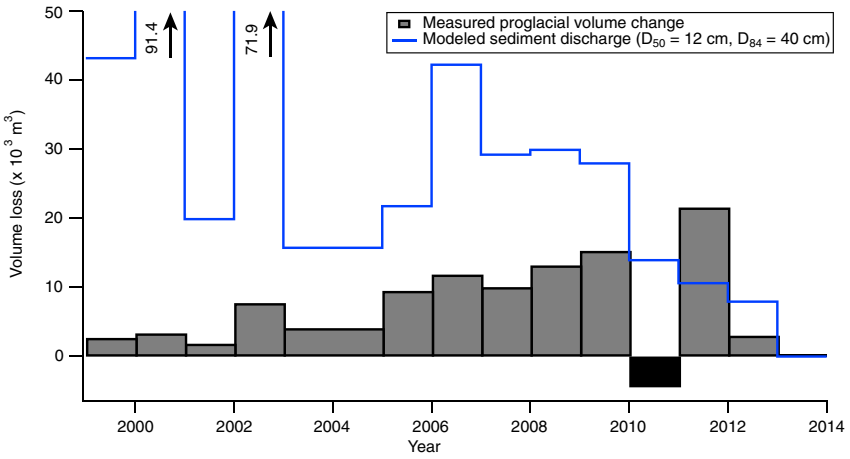

Figure 8. Sediment transport, determined by methods discussed in the text. [Colour figure can be viewed at wileyonlinelibrary.com]

the supply of transportable sediment. In the process, either leaving the sediment in the channel bed too large for fluvial transport or eroding sediment to bedrock. Interestingly, substantial deposition occurs on the shallower reaches following steeper sections (Figure 6), likely a result of water losing the energy required to transport sediment from the upper proglacial area to the lower proglacial area.

Although possibly attributable to the role of debris-covered ice melt in the proglacial area, the poor relationship between observed and modeled sediment erosion (Figure 8), along with the observation of stabilized channel reaches (Figure 6) and a weakening gradient between sediment and water discharge (Figure 7), suggests stabilization and reduced erosion in the proglacial area. As discussed in Lane *et al.* (2016), this could be due to gully formation, sorting of glacial till and removal of transportable sediment. Each of the three pieces of evidence show different time frames over which such processes could have occurred. The bedload transport modeling correlated poorly across most years, suggesting that sediment supply could have been limited prior to 2000 and the uncovering of the proglacial area by the glacier. However, this observation is limited by the poorly constrained grain size. Stabilization of profile reaches, beginning in 2007, show that erosion relaxed in some places prior to that year, while the weakening gradient observed in Figure 7 occurred as late as 2010 or 2013. Despite differences in time frame, these examples show that stabilization can begin on timescales of less than 15 years from deglaciation, and following responses, although relevant (e.g. Curry *et al.*, 2006), are of reduced importance (Ballantyne, 2002b; Lane *et al.*, 2016; Carrivick and Heckmann, 2017).

Sediment sources and erosion rates

Proglacial reservoirs and lakes capture much of the sediment expelled from glaciers and thus serve as a sediment sink (e.g. Bogen, 1989; Geilhausen *et al.*, 2013), and the reduction in reservoir or lake volume, particularly in recent decades, is substantial (Anselmetti *et al.*, 2007). As quantification of changes to reservoir volume is of utmost interest for the hydropower operators who utilize Griessee, bathymetry has been collected for several years (1976, 2011, 2013, 2014). These data enable quantification of sedimentation rates in the Griesgletscher's catchment (internal reports; OFIMA, 2015); however, over the 35 years from 1975 to 2011, climatic changes undoubtedly occurred that could lead to large decadal and interannual variability in sediment input into the lake (e.g., Micheletti and Lane, 2016). As some years experience net annual deposition in the proglacial area, e.g. 2011, at least some sediment must originate subglacially.

For the analyses below it is assumed that no sediment leaves the reservoir, as the water expelled from the turbine during winter of 2015–16 exhibited average sediment concentrations of less than 4 mg L^{-1}, resulting only about 265 m^3 of sediment leaving the catchment (internal unpublished data). Additionally, it is assumed that all material that leaves the proglacial area is sediment and not ice. To account for bulk density changes between the proglacial sediment and the reservoir sediment, we assume that the density of sediment accounted in our DEM analysis is 1 700 kg m^{-3} (Curry *et al.*, 2009). Using grain-size distributions of sediment samples collected from the bottom of Griessee during summer 2015 (personal communication, D. Ehrbar, 2016) the Lara–Pemberton relationship was used to determine bulk density of 1270 kg m^{-3} for sediments deposited in the lake (Morris and Fan, 1998).

Between 1976 and 2011, 618 200 m^3 of sediment was deposited in the reservoir, averaging 17 700 m^3 a^{-1} (Table II). This influx of material far exceeds 3 650 m^3 a^{-1}, the net annual proglacial erosion from 1986 to 2011, suggesting that a maximum of 72% of total sediment deposited in the reservoir originates from subglacial sources, or from other parts of the catchment, routed through the subglacial hydraulic system. However, given the annual resolution of the DEMs, an unknown amount of proglacial sediment was surely deposited in the reservoir and potentially replenished by subglacial sediment, leading to a systematic underestimation of sediment leaving the proglacial area. The next bathymetry, taken in 2013, suggests that 197 550 m^3 of sediment was deposited in the reservoir since 2011 – nearly a third of the amount deposited in the 35 years from 1976 to 2011. Although 2012 experienced the greatest amount of proglacial erosion over the study period, the discrepancy between the eroded volume from the proglacial area and the loss of reservoir volume, between 2011 and 2013, shows that proglacial erosion could be responsible for under 20% of the observed decrease in reservoir volume (Table III). Although in 2013 the proglacial area experienced a marginal amount of net erosion, and the measured amount is underestimated, these results suggest a large amount of subglacial erosion occurred during this year.

The difference in bathymetry from 2014 and 2013 data suggests that only 12 400 m^3 of sediment was deposited in the reservoir over that time period, an amount below the average from 1976 to 2011. Proglacial volume changes were slightly negative during 2014 (Figure 3), which supports minimal sed-

Table III. Bathymetry results for the reservoir (res.) and catchment erosion rates (ΔH) for the proglacial area (PGA) and catchment (catch.).

Time span	ΔVol. res. (m^3)	ΔVol. res. ($m^3\ a^{-1}$)	ΔVol. PGA ($m^3\ a^{-1}$)	% Vol. catch.	ΔH PGA ($cm\ a^{-1}$)	ΔH catch. ($cm\ a^{-1}$)
1976–2011	−618 240	−17 660	—	—	—	−0.08
1986–2011	—	—	−3 650	72%	−6.20	—
2011–2013	−197 550	−98 780	−12 030	84%	−6.26	−0.46
2013–2014	−12 370	−12 370	−190	98%	−0.01	−0.03
1976(86)–2014	−828 240	−21 800	−4 490	72%	−5.96	−0.10

Note: Percentages calculated and height changes assume a density of sediments in reservoir of 1270 $kg\,m^{-3}$, PGA density of 1700 $kg\,m^{-3}$ and density of bedrock in the catchment of 2650 $kg\,m^{-3}$. Additionally, years experiencing deposition are excluded from the calculation. Time periods are based upon the coincident collection of bathymetry data and imagery. In April 2013 a reservoir flushing took place and an estimated 36 000 m^3 of sediment escaped the reservoir (personal communication, G. Köppel, 2015).

iment input into the reservoir from proglacial sources. Over the time span covered with our data from 1976 (bathymetry) and 1986 (DEMs) until 2014, a maximum of 72%, due to systematic bias, of sediment deposited in the reservoir either originated subglacially or was eroded elsewhere in the catchment and passed through the subglacial system to the lake (Table III). This amount is comparable to ratios found by Guillon *et al.* (2015) (50–90%) and by Fenn and Gomez (1989), who suggest that a majority of sediment originates subglacially.

Volumetric changes in the reservoir, deduced by the bathymetries, can be used to determine specific erosion rates in the catchment. The catchment area was considered to be 10.3 km^2 (including a non-glaciated sub-catchment draining from the east and the reservoir); additionally, density of sediment in the reservoir was translated to bedrock density (2 650 $kg\,m^{-3}$). Effective erosion rates for the entire catchment were roughly 1 $mm\,a^{-1}$ over the study period, being over four times higher from 2011 to 2013 (Table III). This value corresponds to studies by Hallet *et al.* (1996) and Anselmetti *et al.* (2007), who estimate erosion rates in the Swiss Alps to be 0.097 and 0.094 $cm\,a^{-1}$, respectively, with some catchments experiencing rates up to 0.17 $cm\,a^{-1}$ (Hallet *et al.*, 1996).

Effective erosion rates (height changes) in the proglacial area over the study period are roughly 40 times that of the catchment as a whole, assuming the density of bedrock for both regions. This substantial difference in specific erosion rate between the proglacial area and whole catchment demonstrates the propensity for proglacial areas to serve as a massive sediment sources should large amounts of unconsolidated sediment be exposed, although retreat of a glacier does not necessarily result in the exposure of unconsolidated sediment, as is the case for the nearby Rhonegletscher which terminates on bedrock, or proglacial lakes, which can serve as sediment traps (e.g. Geilhausen *et al.*, 2013; Bogen *et al.*, 2014).

However, greater quantities of sediment originate subglacially than from the proglacial area. As glaciers retreat and periglacial areas expand, glaciers could lose their erosive potential. This comes as a result of thinner ice, which results in decreased subglacial water pressures, in turn reducing shear stress between water and the bed of the glacier, and thus limiting sediment transport (e.g. Fowler and Walder, 1994). Thus, the relative contribution of subglacial and periglacial sources will evolve; however, speculation regarding the relative contributions of the respective sediment sources in the future will require tools not addressed by this study.

Estimating infill time of Griessee provides some context to sedimentation rates over the study period (e.g. Anselmetti *et al.*, 2007). The bathymetry of 2014 yielded a reservoir volume of 18.64×10^6 m^3 given a spillway crest of 2386.5 m a.s.l. Using annual sedimentation rates from 1976 to 2014 (Table III) yields a reservoir infill time of more than 850 years, not accounting for the effects of sediment compaction. Use of other sedimentation rates determined from comparison of other time periods (Table III) suggests infill times ranging from 190 to 1 500 years for Griessee.

These infill times assume a steady sediment input. However, in addition to the changing contributions and processes of the subglacial and periglacial sources, radar measurements indicate a small over-deepening near the glacier's tongue (Feiger *et al.*, 2017), which could currently moderate the amount of subglacial sediment being expelled from the glacier (Alley *et al.*, 2003; Cook and Swift, 2012; Creyts *et al.*, 2013). Retreat of the glacier beyond the over-deepening will likely create a proglacial lake, which could serve as a sink for water leaving the glacial (e.g. Bogen, 1989; Geilhausen *et al.*, 2013). Additionally, further retreat of the glacier reduces the slope of the proglacial area, thus minimizing the erosive capacity of water flowing through the proglacial area (e.g. Meyer-Peter and Müller, 1948; Rickenmann, 2001).

Conclusions and Future Implications

Aerial photos of Griesgletscher from 1986 to 2014 were used to create DEMs of the proglacial area at an annual resolution. Retreat of the glacier beyond the reservoir margin exposed the proglacial area in 1986, and it grew to over 0.21 km^2 by 2014, providing an ample area for sediment to be eroded and deposited. Analysis of the DEMs spanning the 28 years suggests that 125 600 m^3 of material was removed from the proglacial area over this time and not replenished. Cross-sections of the proglacial area show that much erosion occurred at the bottom of channels, and wall collapse due to ice melt or over-steepening could supply sediment to channel bottoms, where it could be transported out of the proglacial area fluvially. Erosion volumes have increased since the late 1990s; however, annual amounts of erosion decreased in the last 3–4 years of the study, indicating that the proglacial area might have begun to stabilize.

Three observations indicate that the availability of sediment for removal by fluvial activity is limited. (1) Stable areas along steep reaches in channel profiles (Figure 6) suggest that higher slopes have increased erosion of available sediment (e.g. Meyer-Peter and Müller, 1948; Rickenmann, 2001). (2) Poor correlation and potential overestimation of modeled sediment discharge compared to measured quantities suggest that more sediment could be transported by fluvial means than is available for transport (Figure 8). (3) The gradient in the relationship between sediment and discharge has relaxed in recent years

(Figure 7), consistent with limited sediment sources. This is likely due in part to sediment sorting and exhaustion of transportable material in channel bottoms, where water flows. (e.g. Lane *et al.*, 2016), and reduced slope of the proglacial area. As a result, much of the current sediment eroded must come from very recently exposed surfaces, or from collapse of channel walls due to over-steepening. However, comparison of these various observation fail to agree on an exact time frame over which sediment supply became limited.

Comparison of bathymetric data to determine total catchment erosion with volume changes from the proglacial area suggests that more than 70% of sediment deposited in the reservoir originates subglacially or from other parts of the catchment. However, denudation rates in the proglacial area are far higher than those in the rest of the catchment: −3.8 and −0.1 cm a^{-1}. As the glacier thins, water pressure, partially responsible for activating subglacial sediments, will decrease (e.g. Fowler and Walder, 1994), diminishing the erosive capacity of the glacier (e.g. Koppes *et al.*, 2010). Although the proglacial area will increase in size, the sediment dynamics will likely change, as runoff is expected to lessen after roughly 2020 (Farinotti *et al.*, 2012). Thus the current contribution of subglacial and proglacial sediment to the total catchment sediment budget will need to be reconciled with the competing processes, along with proper attention to proglacial sediment availability. Additionally, small amounts of vegetation have begun to grow in the proglacial area, which can develop soils and enable yet more vegetation to exist, further stabilizing slopes (Ballantyne, 2002a; Sigler *et al.*, 2002). The glacier is expected almost to disappear by the end of this century (Farinotti *et al.*, 2012), leaving fluvial and periglacial processes solely responsible for the catchment's sediment dynamics.

Finding ways to partition subglacial and proglacial erosion at a higher temporal resolution would prove fruitful in describing sedimentation in glaciated catchments (e.g. Fenn and Gomez, 1989; Guillon *et al.*, 2015). In particular, as a large fraction of material originates from below the glacier, a better understanding of sedimentation in Griesgletscher's catchment requires more thorough characterization of subglacial erosion. Additionally, further parametrizing of sub- and periglacial erosion with respect to glaciological and climatological data will enable forecasts of sediment transport for the coming years as the hydrology and ice coverage of glaciated catchments change.

Acknowledgements—

This work was funded by the Swiss National Science Foundation (SNSF) National Research Programme (NRP) 70 'Energy Turnaround', Project No. 153927. We thank G. Köppel and hydropower operators KW Aegina and OFIMA for their logistical support and use of both runoff data to calibrate our melt model and reservoir bathymetry data. We also thank R.B.R. Geophysics GmbH for their technical support with collection of bathymetry data. M. Rothermel and M. Detert made many useful suggestions regarding the photogrammetry. M. Raymond-Pralong helped us implement the sediment modeling. D. Ehrbar provided useful discussions with regard to bathymetry data and reservoir processes, and M. Funk commented on an earlier version of the manuscript. Lastly, three anonymous reviewers greatly improved this manuscript.

References

Alley R, Cuffey K, Evenson E, Strasser J, Lawson D, Larson G. 1997. How glaciers entrain and transport basal sediment: physical constraints. *Quaternary Science Reviews* **16**: 1017–1038.

Alley R, Lawson D, Larson G, Evenson E, Bake G. 2003. Stabilizing feedbacks in glacier-bed erosion. *Nature* **424**: 758–760.

Anselmetti F, Bühler R, Finger D, Girardclos S, Lancini A, Rellstab C, Sturm M. 2007. Effects of alpine hydropower dams on particle transport and lacustrine sedimentation. *Aquatic Sciences* **69**: 179–198.

Auel C, Boes R. 2012. *Sustainable reservoir management using sediment bypass tunnels*: London, 224–241.

Ballantyne C. 2002a. A general model of paraglacial landscape response. *The Holocene* **12**: 371–376.

Ballantyne C. 2002b. Paraglacial geomorphology. *Quaternary Science Reviews* **21**: 1935–2017.

Baltsavias E. 1999. A comparison between photogrammetry and laser scanning. *ISPRS Journal of Photogrammetry and Remote Sensing* **54**: 83–94.

Bauder A, Funk M, Huss M. 2007. Ice-volume changes of selected glaciers in the Swiss Alps since the end of the 19th century. *Annals of Glaciology* **46**: 145–149.

Beaud F, Flowers G, Venditti J. 2016. Efficacy of bedrock erosion by subglacial water flow. *Earth Surface Dynamics Discussions* **3**: 849–908.

Bennett M, Huddart D, Glasser N, Hambrey M. 2000. Resedimentation of debris on an ice-cored lateral moraine in the high-Arctic (Kongsvegen, Svalbard). *Geomorphology* **35**: 21–40.

Betts H, Trustrum N, Rose RD. 2003. Geomorphic changes in a complex gully system measured from sequential digital elevation models, and implications for management. *Earth Surface Processes and Landforms* **28**: 1043–1058.

Bogen J. 1989. Glacial sediment production and development of hydroelectric power in glacierized areas. *Annals of Glaciology* **13**: 6–11.

Bogen J, Xu M, Kennie P. 2014. The impact of pro-glacial lakes on downstream sediment delivery in Norway. *Earth Surface Processes and Landforms* **40**: 942–952.

Bolstad P. 1992. Geometric errors in natural resource GIS data: Tilt and terrain effects in aerial photographs. *Forest Science* **38**: 367–380.

Carrivick J, Heckmann T. 2017. Short-term geomorphological evolution of proglacial systems. *Geomorphology* **287**: 3–28.

Church M, Ryder J. 1972. Paraglacial sedimentation: A consideration of fluvial processes conditioned by glaciation. *Geological Society of America Bulletin* **83**: 3059–3072.

Cook SJ, Swift DA. 2012. Subglacial basins: Their origin and importance in glacial systems and landscapes. *Earth-Science Reviews* **115**: 332–372.

Creyts T, Clarke GK, Church M. 2013. Evolution of subglacial overdeepenings in response to sediment redistribution and glaciohydraulic supercooling. *Journal of Geophysical Research: Earth Surface* **118**: 423–446.

Curry A, Cleasby V, Zukowskyj P. 2006. Paraglacial response of steep, sediment-mantled slopes to post-Little Ice Age glacier recession in the central Swiss Alps. *Journal of Quaternary Science* **21**: 211–225.

Curry A, Sands T, Porter P. 2009. Geotechnical controls on a steep lateral moraine undergoing paraglacial slope adjustment. *Geological Society, London, Special Publications* **320**: 181–197.

Einsele G, Hinderer M. 1997. Terrestrial sediment yield and the lifetimes of reservoirs, lakes, and larger basins. *Geologische Rundschau* **86**: 288–310.

Eyles N. 1979. Facies of supraglacial sedimentation on Icelandic and Alpine temperate glaciers. *Canadian Journal of Earth Sciences* **16**: 1341–1361.

Fabris M, Pesci A. 2005. Automated DEM extraction in digital aerial photogrammetry: precisions and validation for mass movement monitoring. *Annals of Geophysics* **48**: 973–988. https://doi.org/10.4401/ag-3247.

Farinotti D, Usselmann S, Huss M, Bauder A, Funk M. 2012. Runoff evolution in the Swiss Alps: projections for selected high-alpine catchments based on ENSEMBLES scenarios. *Hydrological Processes* **26**: 1909–1924.

Feiger N, Huss M, Leinss S, Sold L, Farinotti D. 2017. An updated bedrock topography for Gries- and Findelengletscher. Geographica Helvetica (submitted for publication).

Felix D, Albayrak I, Boes R. 2013. Laboratory investigation on measuring suspended sediment by portable laser diffractometer (LISST) focusing on particle shape. *Geo-Marine Letters* **33**: 485–498.

Fenn C, Gomez B. 1989. Particle size analysis of the sediment suspended in a proglacial stream: Glacier de Tsidjiore Nouve, Switzerland. *Hydrological Processes* **3**: 123–135.

Fischer U, Braun A, Bauder A, Flowers G. 2005. Changes in geometry and subglacial drainage derived from digital elevation models: Unteraargletscher, Switzerland, 1927–97. *Annals of Glaciology* **40**: 20–24.

Fowler A, Walder J. 1994. Channelized subglacial drainage over a deformable bed. *Journal of Glaciology* **40**: 3–15.

Geilhausen M, Morche D, Otto J, Schrott L. 2013. Sediment discharge from the proglacial zone of a retreating Alpine glacier. *Zeitschrift für Geomorphologie Supplementary Issue* **57**: 29–53.

Glasser N, Holt T, Evans Z, Davies B, Pelto M, Harrison S. 2016. Recent spatial and temporal variations in debris cover on Patagonian glaciers. *Geomorphology* **273**: 202–216.

Guillon H, Mugnier J, Buoncristiani J, Carcaillet J, Godon C, Prud'homme C, Beek P, Vassallo R. 2015. Improved discrimination of subglacial and periglacial erosion using ^{10}Be concentration measurements in subglacial and supraglacial sediment load of the Bossons glacier (Mont Blanc Massif, France). *Earth Surface Processes and Landforms* **40**: 1202–1215.

Hallet B, Hunter L, Bogen J. 1996. Rates of erosion and sediment evacuation by glaciers: a review of field data and their implications. *Global and Planetary Change* **12**: 213–235.

Herman F, Beyssac O, Brughelli M, Lane S, Leprince S, Adatte T, Lin J, Avouac JP, Cox S. 2015. Erosion by an Alpine glacier. *Science* **350**: 193–195.

Hinderer M, Kastowski M, Kamelger A, Bartolini C, Schlunegger F. 2013. River loads and modern denudation of the Alps: A review. *Earth-Science Reviews* **118**: 11–44.

Hock R. 1999. A distributed temperature-index ice- and snowmelt model including potential direct solar radiation. *Journal of Glaciology* **45**: 101–111.

Hoelzle M, Haeberli W. 1995. Simulating the effects of mean annual air temperature changes on permafrost distribution and glacier size: an example from the Upper Engadin, Swiss Alps. *Annals of Glaciology* **21**: 399–405.

Hubbard A, Willis I, Sharp M, Mair D, Nienow P, Hubbard B, Blatter H. 2000. Glacier mass-balance determination by remote sensing and high resolution modelling. *Journal of Glaciology* **46**: 491–498.

Huss M. 2012. Extrapolating glacier mass balance to the mountain range scale: the European alps 1900–2100. *The Cryosphere* **6**: 1117–1156.

Huss M, Farinotti D, Bauder A, Funk M. 2008. Modelling runoff from highly glacierized alpine drainage basins in a changing climate. *Hydrological Processes* **22**: 3888–3902.

Huss M, Bauder A, Funk M. 2009. Homogenization of long-term mass balance time series. *Annals of Glaciology* **50**: 198–206.

Huss M, Dhulst L, Bauder A. 2015. New long-term mass-balance series for the Swiss Alps. *Journal of Glaciology* **61**: 551–562.

James M, Robson S. 2012. Straightforward reconstruction of 3D surfaces and topography with a camera: accuracy and geoscience application. *Journal of Geophysical Research: Earth Surface* **117**((F3)). https://doi.org/10.1029/2011JF002289.

Kenner R, Bühler Y, Delaloye R, Ginzler C, Phillips M. 2014. Monitoring of high alpine mass movements combining laser scanning with digital airborne photogrammetry. *Geomorphology* **206**: 492–504.

Koppes M, Montgomery D. 2009. The relative efficacy of fluvial and glacial erosion over modern to orogenic timescales. *Nature Geoscience* **2**: 644–647.

Koppes M, Hallet B, Anderson J. 2009. Synchronous acceleration of ice loss and glacial erosion, Glaciar Marinelli, Chilean Tierra del Fuego. *Journal of Glaciology* **55**: 207–220.

Koppes M, Sylwester R, Rivera A, Hallet B. 2010. Variations in sediment yield over the advance and retreat of a calving glacier, Laguna San 890 Rafael, North Patagonian Icefield. *Quaternary Research* **73**: 84–95.

Lane S, Bakker M, Gabbud C, Micheletti N, Saugy J. 2016. Sediment export, transient landscape response and catchment-scale connectivity following rapid climate warming and alpine glacier recession. *Geomorphology* **277**: 210–227.

Legg N, Meigs A, Grant G, Kennard P. 2014. Debris flow initiation in proglacial gullies on Mount Rainier, Washington. *Geomorphology* **226**: 249–260.

Leggat M, Owens P, Stott T, Forrester B, Déry S, Menounos B. 2015. Hydro-meteorological drivers and sources of suspended sediment flux in the pro-glacial zone of the retreating Castle Creek Glacier, Cariboo Mountains, British Columbia, Canada. *Earth Surface Processes and Landforms* **40**: 1542–1559.

Lundstrom S, McCafferty A, Coe J. 1993. Photogrammetric analysis of 1984–89 surface altitude change of the partially debris-covered Eliot glacier, Mount Hood, Oregon, USA. *Annals of Glaciology* **17**: 167–170.

Mao L, Dell'Agnese A, Huincache C, Penna D, Engel M, Niedrist G, Comiti F. 2014. Bedload hysteresis in a glacier-fed mountain river. *Earth Surface Processes and Landforms* **39**: 964–976.

Meigs A, Krugh W, Davis K, Bank G. 2006. Ultra-rapid landscape response and sediment yield following glacier retreat, Icy Bay, southern Alaska. *Geomorphology* **78**: 207–221.

Meyer-Peter E, Müller R. 1948. *Formulas for bed-load transport*, Hydraulic Engineering Reports. IAHR: Madrid.

Micheletti N, Lane S. 2016. Water yield and sediment export in small, partially glaciated alpine watersheds in a warming climate. *Water Resources Research* **52**: 4924–4943.

Micheletti N, Lambiel C, Lane S. 2015. Investigating decadal-scale geomorphic dynamics in an alpine mountain setting. *Journal of Geophysical Research: Earth Surface* **120**: 2155–2175.

Montgomery D, Dietrich W. 1994. A physically based model for the topographic control on shallow landsliding. *Water Resources Research* **30**: 1153–1171.

Morris G, Fan J. 1998. *Reservoir Sedimentation Handbook: Design and Management of Dams, Reservoirs, and Watersheds for Sustainable Use*. McGraw Hill Professional: New York.

Nicholson L, Benn D. 2006. Calculating ice melt beneath a debris layer using meteorological data. *Journal of Glaciology* **52**: 463–470.

Nuth C, Kääb A. 2011. Co-registration and bias corrections of satellite elevation data sets for quantifying glacier thickness change. *The Cryosphere* **5**: 271–290.

Paul F, Huggel C, Kääb A. 2004. Combining satellite multispectral image data and a digital elevation model for mapping debris-covered glaciers. *Remote sensing of Environment* **89**: 510–518.

Porter P, Vatne G, Ng F, Irvine-Fynn TD. 2010. Ice-marginal sediment delivery to the surface of a high-Arctic glacier: Austre Brøggerbreen, Svalbard. *Geografiska Annaler: Series A, Physical Geography* **92**: 437–449.

Raymond-Pralong M, Turowski J, Rickenmann D, Zappa M. 2015. Climate change impacts on bedload transport in alpine drainage basins with hydropower exploitation. *Earth Surface Processes and Landforms* **40**: 1587–1599.

Reinhardt W, Rentsch H. 1986. Determination of changes in volume and elevation of glaciers using digital elevation models for the Vernagtferner, Ötztal Alps, Austria. *Annals of Glaciology* **8**: 151–158.

Rickenmann D. 2001. Comparison of bed load transport in torrents and gravel bed streams. *Water Resources Research* **37**: 3295–3305.

Rickenmann D, Recking A. 2011. Evaluation of flow resistance in gravel bed rivers through a large field data set. *Water Resources Research* **47**. https://doi.org/10.1029/2010WR009793.

Rippin D, Willis I, Arnold N, Hodson A, Moore J, Kohler J, Björnsson H. 2003. Changes in geometry and subglacial drainage of Midre Lovénbreen, Svalbard, determined from digital elevation models. *Earth Surface Processes and Landforms* **28**: 273–298.

Rolstad C, Haug T, Denby B. 2009. Spatially integrated geodetic glacier mass balance and its uncertainty based on geostatistical analysis: application to the western Svartisen ice cap, Norway. *Journal of Glaciology* **55**: 666–680.

Röthlisberger H. 1972. Water pressure in intra? and subglacial channels. *Journal of Glaciology* **11**: 177–203.

Schaefli B, Hingray B, Musy A. 2007. Climate change and hydropower production in the Swiss Alps: quantification of potential impacts and related modelling uncertainties. *Hydrology and Earth System Sciences Discussions* **11**: 1191–1205.

Schiefer E, Gilbert R. 2007. Reconstructing morphometric change in a proglacial landscape using historical aerial photography and automated DEM generation. *Geomorphology* **88**: 167–178.

Schiefer E, Menounos B, Wheate R. 2007. Recent volume loss of British Columbian glaciers, Canada. *Geophysical Research Letters* **34**: 167–178. https://doi.org/10.1029/2007GL030780.

Schomacker A, Kjær K. 2008. Quantification of dead-ice melting in ice-cored moraines at the high-arctic glacier holmströmbreen, Svalbard. *Boreas* **37**: 211–225.

Sigler W, Crivii S, Zeyer J. 2002. Bacterial succession in glacial fore-field soils characterized by community structure, activity and opportunistic growth dynamics. *Microbial Ecology* **44**: 306–316.

Stott T, Mount N. 2007. Alpine proglacial suspended sediment dynamics in warm and cool ablation seasons: Implications for global warming. *Journal of Hydrology* **332**: 259–270.

Swift D, Nienow P, Hoey T. 2005. Basal sediment evacuation by subglacial meltwater: suspended sediment transport from Haut Glacier d'Arolla, Switzerland. *Earth Surface Processes and Landforms* **30**: 867–883.

Warburton J. 1990. An alpine proglacial fluvial sediment budget. *Geografiska Annaler: Series A, Physical Geography* **72**: 261–272.

Werder M, Bauder A, Funk M, Keusen H. 2010. Hazard assessment investigations in connection with the formation of a lake on the tongue of Unterer Grindelwaldgletscher, Bernese Alps, Switzerland. *Natural Hazards and Earth System Science* **10**: 227–237.

